European Journal of Pharmaceutical Sciences 77 (2015) 40–47

Contents lists available at ScienceDirect

European Journal of Pharmaceutical Sciences

journal homepage: www.elsevier.com/locate/ejps

Gastrointestinal behavior of nano- and microsized fenofibrate: *In vivo* evaluation in man and *in vitro* simulation by assessment of the permeation potential

Bart Hens [a,1], Joachim Brouwers [a,1], Maura Corsetti [b], Patrick Augustijns [a,*]

[a] Drug Delivery & Disposition, KU Leuven, Gasthuisberg O&N2, Herestraat 49, Box 921, 3000 Leuven, Belgium
[b] Translational Research Center for Gastrointestinal Disorders (TARGID), KU Leuven, Belgium

ARTICLE INFO

Article history:
Received 20 March 2015
Received in revised form 20 May 2015
Accepted 20 May 2015
Available online 21 May 2015

Keywords:
Dissolution
Permeation
Solubility–permeability interplay
Fenofibrate
Nanoparticles
Microparticles
Dialysis
Clinical study

ABSTRACT

Introduction: The purpose of this study was (i) to evaluate the gastrointestinal behavior of micro- and nanosized fenofibrate in humans and (ii) to develop a simple yet qualitatively predictive *in vitro* setup that simulates the observed absorption-determining factors.
Materials and methods: Commercially available micro- and nanoparticles of fenofibrate (Lipanthyl® and Lipanthylnano®, respectively) were administered orally to five healthy volunteers in fasting and postprandial conditions. Intraluminal and systemic drug concentrations were determined as reference data for the development of a predictive *in vitro* setup. To capture the observed solubility/permeability interplay, *in vitro* dissolution testing was performed in the presence of a permeation bag with sink conditions.
Results: In fasting conditions, intake of nanosized fenofibrate generated increased duodenal concentrations compared to microsized fenofibrate, which was reflected in an improved systemic exposure. In postprandial conditions, duodenal concentrations were greatly enhanced for both formulations, however without an accompanying increase in systemic exposure. It appeared that micellar encapsulation of the highly lipophilic fenofibrate limited its potential to permeate from fed state intestinal fluids. To capture these *in vivo* observations in an *in vitro* setup, classic dissolution testing was combined with permeation assessment into a permeation bag with sink conditions. In case of fasting conditions, the dissolution/permeation approach allowed for an improved discriminative power between micro- and nanosized fenofibrate by better simulating the dynamic interplay of dissolution and absorption. In case of postprandial conditions, the observed solubility–permeability interplay could be simulated using the dissolution/permeation approach in combination with biorelevant media ($FeSSGF_{Fortimel}$ and FeSSIF-V2) to mimic micellar entrapment and reduced permeation potential of fenofibrate.
Conclusion: For the first time, reduced permeation of a lipophilic drug despite increased intraluminal concentrations, was demonstrated in humans. Dissolution testing using biorelevant media in combination with permeation assessment into a sink permeation bag appeared to be a simple yet pragmatic approach to capture this solubility–permeability interplay in early formulation evaluation.

1. Introduction

Over the past decades, the number of drug discovery compounds has increased tremendously: advanced technologies (i.e. high throughput screening and combinatorial chemistry) allow screening of a wide range of new molecular entities for their pharmacodynamic activity in the shortest possible time. However, the oral absorption potential of drug candidates selected using these techniques is often compromised by suboptimal biopharmaceutical properties, including low aqueous solubility and poor dissolution kinetics (Biopharmaceutical Classification System 2 and 4) (Benet et al., 2011; Lipinski, 2000; Amidon et al., 1995). To increase the oral bioavailability of poorly water soluble drugs, absorption-enabling formulation strategies are often required, including the use of solubilizing excipients (cyclodextrins, surfactants and lipids), (amorphous) solid dispersions, crystalline salt forms, prodrugs and particle size reduction (Brouwers et al., 2009; Williams et al., 2013).

* Corresponding author at: Drug Delivery & Disposition, Campus Gasthuisberg O&N 2, Box 921, Herestraat 49, 3000 Leuven, Belgium.
E-mail address: patrick.augustijns@pharm.kuleuven.be (P. Augustijns).
[1] These authors should both be considered as first author.

http://dx.doi.org/10.1016/j.ejps.2015.05.023
0928-0987/

In this respect, micro- and nanonization of poorly soluble compounds is an attractive strategy to increase their dissolution rate (Van Eerdenbrugh et al., 2010). Although particle size reduction often exerts a positive effect on oral bioavailability, the exact behavior of micro- and nanoparticles in the gastrointestinal tract remains to be studied. In order to predict the *in vivo* performance of these formulations, single phasic *in vitro* dissolution tests are still the norm (Nakarani et al., 2010; Wang et al., 2010). However, the predictive power of these simple setups is limited, since they do not fully capture the interplay between crucial gastrointestinal processes (e.g. secretions, pH, volumes, gastrointestinal transfer and intestinal absorption) and their influence on the performance of micro- and nanoparticles. For instance, Sigfridsson et al. demonstrated no difference in plasma concentration of the basic compound BA99 in rats, formulated as a micro- or nanosuspension (i.e. 12 μm versus 280 nm particle size, respectively) (Sigfridsson et al., 2011); only two-stage dissolution testing in a gastric and intestinal compartment could demonstrate that the high gastric solubility of BA99 limits the need of particle size reduction in order to increase oral bioavailability.

In this study, we used the neutral compound fenofibrate as a model compound. Fenofibrate (logP 5.21) is a typical lipophilic BCS class 2 compound, suffering from a poor aqueous solubility, which results in a low systemic exposure after oral administration. In order to overcome this hurdle, fenofibrate is on the market as micro- and nanoparticles (Lipanthyl® and Lipanthylnano®, respectively). By combining dissolution experiments with physiological-based pharmacokinetic (PBPK) modelling, Juenemann et al. clearly demonstrated that, in fasting conditions, the higher dissolution rate for the nanosized formulation results in improved systemic exposure compared to the microsized formulation (Juenemann et al., 2011). In postprandial conditions, drug release from both formulations was increased; however, this was not accompanied with a significantly higher exposure, as confirmed by Sauron et al. (2006). The absence of a positive systemic food effect demonstrates that estimating formulation performance based on simple dissolution experiments does not always capture the key intraluminal processes determining drug absorption from enabling strategies. In order to fully assess the performance of enabling formulations, the absorption-determining intraluminal processes should be identified and integrated into *in vitro* models (Buckley et al., 2013).

Hence, the aim of this study can be subdivided into two major objectives: (i) an in-depth analysis of the gastrointestinal behavior and systemic exposure of micro- and nanosized fenofibrate in fasting and fed conditions in man and (ii) implementing the *in vivo* observations into a predictive yet simple *in vitro* setup, focusing on assessment of permeation potential in addition to dissolution testing.

2. Materials and methods

2.1. Chemicals

Fenofibrate was obtained from Indis (Aartselaar, Belgium). Dimethyl sulfoxide (DMSO), methanol (MeOH) and $NaH_2PO_4{\cdot}H_2O$ were purchased from Acros Organics (Geel, Belgium), while BHD Laboratory Supplies (Poole, UK) supplied HCl, NaOH and maleic acid. PharmInnova (Waregem, Belgium) supplied carbamazepine. Orlistat was purchased from Sigma Aldrich (St. Louis, MO, USA). Acetonitrile, dichloromethane and NaCl were purchased from Fisher Scientific (Leicestershire, UK). Sodium acetate and acetic acid were received from VWR (Leuven, Belgium). Lecithin was supplied by Phospholipid Gmbh (Köln, Germany). Sodium taurocholate was provided by MP Biomedicals LLC (Illkirch, France). Danisco (Ottignies-Louvain-la-Neuve, Belgium) provided glyceryl monooleate. Sodium oleate was kindly supplied by Riedel-de Haën (Seelze-Hannover, Germany). Biorelevant (Croydon, UK) provided simulated intestinal fluid (SIF) powder. Water was purified by using a Maxima system (Elga Ltd., High Wycombe Bucks, UK).

To prepare fasted state simulated intestinal fluid (FaSSIF), containing taurocholate (3 mM) and lecithin (0.75 mM), 2.24 mg SIF powder was dissolved per milliliter FaSSIF buffer (pH 6.5), which contains NaOH (10.5 mM), Na_2HPO_4 (28 mM) and NaCl (106 mM). Fasted state simulated gastric fluid (FaSSGF) was prepared by dissolving 60 mg SIF powder per liter FaSSGF buffer (NaCl 34 mM, pH 1.6). Fortimel-based fed state simulated gastric fluid ($FeSSGF_{Fortimel}$) was prepared by mixing FaSSGF and Fortimel Extra® in a 1:1 ratio and adjusted to pH 5. To prepare FeSSIF-V2 (fed state simulated intestinal fluid version 2), a mixture of sodium taurocholate (10 mM), lecithin (2 mM), glyceryl monooleate (5 mM), sodium oleate (0.8 mM), maleic acid (55.02 mM), NaOH (81.65 mM) and NaCl (125.5 mM) was dissolved in water and adjusted to pH 5.8 (Jantratid et al., 2008).

To simulate the gastrointestinal transfer, 50 ml of FaSSGF was decanted into 150 ml of concentrated FaSSIF (4-fold transfer dilution) to obtain standard concentrations of FaSSIF after transfer. One liter of concentrated FaSSIF was prepared by dissolving 0.56 g NaOH, 5.27 g $NaH_2PO_4{\cdot}H_2O$ and 8.25 g NaCl in 0.9 l purified water. Subsequently, 2.99 g SIF powder was added. The pH was adjusted to 6.5 by using 2 M NaOH and, subsequently, the volume was adjusted to 1 l. To simulate the gastrointestinal transfer from $FeSSGF_{Fortimel}$ to FeSSIF-V2, 50 ml of $FeSSGF_{Fortimel}$ was decanted into 150 ml of FeSSIF-V2 (4-fold transfer dilution).

2.2. In vivo study

Duodenal concentrations of fenofibrate along the gastrointestinal tract were monitored in five healthy volunteers (three men, two women; aged between 23 and 25 years). Gastric concentrations were determined in healthy volunteer 1 (HV 1). Exclusion criteria for volunteer selection included gastrointestinal disorders, infection with hepatitis B, hepatitis C or HIV, the use of medication, pregnancy and frequent X-ray exposure. The study procedure was in accordance with the Declaration of Helsinki and approved by the Committee of Medical Ethics of the University Hospitals Leuven, Belgium (ML9962) and the Federal Agency for Medicines and Health Products (631710). All volunteers provided written informed consent before participating in this study.

After an overnight fasting period of at least 12 h, volunteers arrived at the hospital. A double-lumen polyvinyl catheter [Salem Sump Tube 14 Ch (external diameter 4.7 mm), Covidien, Dublin, Ireland] was introduced via the mouth or nose and positioned into the duodenum (D2/D3); in HV 1, a second catheter was positioned in the antrum (in front of the pylorus). Positioning was checked by fluoroscopy. In addition to intraluminal sampling, blood samples were collected and analyzed for fenofibric acid (active metabolite).

Fenofibrate was administered as microsized and nanosized formulations in the fasted as well as in the fed state using a cross-over design. In case of fasting conditions, 1 capsule of 200 mg microsized fenofibrate (Lipanthyl®, Abbott Products N.V., Brussels, Belgium) or 1 tablet of 145 mg nanosized fenofibrate (Lipanthylnano®, Abbott Products N.V., Brussels, Belgium) was administered with 250 ml of tap water. In fed state conditions, 400 ml of Fortimel Extra® nutrient shake (Nutricia Belgium, Strombeek-Bever, Belgium) was given orally 20 min prior to administration of the micro- or nanosized formulation. The energy value of this liquid meal is 2520 kJ/600 kcal (proteins 26.7%, carbohydrates 41.3%, and lipids 32%). The pH is 6.6 and the osmolarity is 470 mOsm/l. During the entire experiment, volunteers were sitting in an upright position. In all conditions, gastrointestinal aspirates

were collected every 10 min in the first hour, and, subsequently, every 15 min up to 230 min. The sampling volume was kept as small as possible (<4 ml per time point). After aspiration of fluids, pH was immediately measured (Hamilton Knick Portamess®, Bonaduz, Switzerland). To prevent lipolysis, collected fed state duodenal fluids were treated with lipase inhibitor (orlistat, final concentration of 1 μM). Aspirates were stored on ice until analysis on the same day (see below). In parallel to the collection of gastrointestinal fluids, venous blood samples were collected in heparinized tubes (BD Vacutainer systems, Plymouth, UK) at 1, 2, 3, 4, 5, 6, 7, 8 and 24 h after drug intake. Immediately after blood collection, samples were centrifuged (2880*g*, 10 min, 4 °C) and the obtained plasma was stored at −26 °C until analysis (see below).

2.3. Bioaccessible fraction determination of fenofibrate in human intestinal fluids

In order to investigate the free, bioaccessible fraction of fenofibrate in the aspirated human intestinal fluids, a permeation experiment was performed for a selected sample set. The setup for this experiment has been described by Holmstock et al. (2013). Briefly, cellulose membrane strips (molecular weight cutoff of 12–14 kDa (±3 nm)) were positioned between donor and acceptor compartments in order to perform permeation experiments using HTD 96b from HTDialysis, LLC (Gales Ferry, CT, US). Four intestinal samples from HV 3 were selected. The donor compartment was filled with 150 μL of each sample ($n = 3$). The acceptor compartment was filled with 150 μL of a phosphate buffer. The osmolarity of the phosphate buffer was adjusted to the osmolarity of the aspirated samples in the donor compartment (Osmometer model 3250 from Advanced Instruments, Inc. (Norwood, MA, USA)). The pH was equalized by use of diluted NaOH or HCl. After 4 h of incubation, samples were taken from the acceptor compartment and analyzed for fenofibrate in order to assess the bioaccessible fraction.

2.4. Two-stage dissolution testing

To assess the dissolution kinetics for both formulations, a two-step dissolution experiment was performed. In a first step, either 1 tablet Lipanthylnano® (145 mg fenofibrate) or the content of 1 capsule Lipanthyl® (200 mg fenofibrate) was added to 50 ml of FaSSGF. After 15 min, samples were taken to determine fenofibrate concentrations and the entire content of the vessel was transferred to 150 ml of concentrated FaSSIF (4-fold dilution). Samples were taken after 5, 15, 30, 45 and 60 min. Similar dissolution experiments were conducted for both formulations using $FeSSGF_{Fortimel}$ and FeSSIF-V2 to mimic fed state conditions, retaining all other experimental conditions.

2.5. Dissolution testing in the presence of a permeation bag

To explore the added value of including an absorption compartment, a permeation bag with sink conditions was included in the dissolution setup. After disintegration for 15 min in 50 ml FaSSGF, the entire volume was decanted into another beaker, containing 150 ml of concentrated FaSSIF and a clamped permeation bag (Cellu Sep H1, regenerated cellulose tubular membrane, cutoff value 50 kDa, Orange Scientific, Braine-l'Alleud, Belgium) containing 5 ml of a solution of the surfactant D-α-tocopheryl polyethylene glycol succinate (2.5% w/v). To improve mixing inside the bag, a gentle airflow of carbogen was introduced inside the bag. No transport of TPGS from the bag into the dissolution vessel was detected; also no adsorption of fenofibrate was observed to any part of the setup (data not shown). At 10, 30 and 60 min, samples were taken from the dissolution vessel (i.e. donor compartment) and from the permeation bag (i.e. acceptor compartment) ($n = 3$; mean ± S.D.).

In case of postprandial conditions, two sets of experiments were performed, i.e. in the absence or presence of the liquid meal Fortimel Extra®. In the first set of experiments, formulations were allowed to disintegrate in 50 ml of FaSSGF for 15 min and, subsequently, decanted into the dissolution vessel containing 150 ml of FeSSIF-V2 and a clamped permeation bag with sink conditions. In a second set of experiments, formulations were allowed to disintegrate in 50 ml of $FeSSGF_{Fortimel}$ for 15 min and, subsequently, decanted into the dissolution vessel, containing 150 ml of FeSSIF-V2 and a clamped permeation bag with sink conditions. The procedure and sampling were similar as described above ($n = 3$; mean ± S.D.).

2.6. Analysis of fenofibrate/fenofibric acid in simulated and human gastrointestinal fluids

To determine fenofibrate and fenofibric acid concentrations in human and simulated gastrointestinal fluids, an HPLC–UV analysis method was developed. After centrifugation of the aspirated gastrointestinal fluids (20,817*g*, 5 min, 37 °C), 800 μl of the supernatant was filtered (PTFE filter media, 0.1 μm pore size, Whatman, Florham Park, NJ, USA). 100 μl of the filtrate was diluted 1:1 with mobile phase (methanol:25 mM acetic acid buffer pH 3.5 (80:20 v/v)) and precipitated protein was removed by centrifugation (20,817*g*, 5 min, 37 °C).

Subsequently, 50 μl of each sample was injected into an HPLC system consisting of an Alliance 2695 separations module and a Novapak C-18 column under radial compression (Waters, Milford, MA, USA); fenofibrate and fenofibric acid were detected at a wavelength of 287 nm (UV spectrum) (Waters 2487 UV Detector). An isocratic run with methanol:25 mM acetic acid buffer pH 3.5 (80:20 v/v) as mobile phase was performed with a flow rate of 1 ml/min to generate a retention time of 5.5 and 11 min for fenofibric acid and fenofibrate, respectively. Following elution of fenofibrate, the column was rinsed during 1 min with acetonitrile:25 mM acetic acid buffer pH 3.5 (75:25 v/v), followed by 2 min with water:25 mM acetic acid buffer pH 3.5 (75:25 v/v) and subsequently re-equilibrated with the mobile phase for 2 min.

Calibration curves were made in mobile phase based on a stock solution of fenofibrate (80 mM) and fenofibric acid (10 mM) in DMSO. For both compounds, linearity was observed between 200 μM and 97 nM. In case of fenofibrate, accuracy and precision errors were less than 3% and 0.3%, respectively, for a concentration of 12.5 μM in FaHIF. At the day of the *in vivo* study, samples were analyzed together with a quality control sample of 50 μM fenofibrate in FaHIF, resulting in a relative standard deviation of less than 8%.

2.7. Analysis of fenofibric acid in plasma

Before HPLC–UV analysis, fenofibric acid (active metabolite) was extracted from plasma samples. 100 μl of a stock solution of the internal standard solution carbamazepine (20 μM in 1 M HCl) was added to 500 μl of plasma. Subsequently, 400 μl of HCl (1 M) was added and vortexed (±10 s) in order to precipitate plasma proteins. To extract fenofibric acid and carbamazepine, 6 ml of dichloromethane was added and samples were shaken for one minute. After centrifugation (2880*g*, 15 min, 4 °C), the water layer was discarded and the organic layer was evaporated under a stream of air until dryness. The residue was dissolved in 1 ml of methanol. Following evaporation, 200 μl of mobile phase was added to the residue and injected into the HPLC system. Carbamazepine and fenofibric acid were detected at a wavelength of 287 nm (Waters 2487 UV Detector). A retention time of 4.5 and

8 min were generated with a flow rate of 1 ml/min for carbamazepine and fenofibric acid, respectively. Running conditions started with acetonitrile:25 mM acetic acid buffer pH 3.5 (50:50 v/v). Acetonitrile concentrations increased up to 60% over 3 min. Following elution of fenofibric acid, the column was rinsed during 2 min with acetonitrile:water (90:10 v/v), followed by 1 min with water:25 mM acetic acid buffer pH 3.5 (75:25 v/v) and subsequently re-equilibrated with the starting conditions (acetonitrile:25 mM acetic acid buffer pH 3.5 (50:50 v/v)) for 2 min.

The calibration curve was based on a stock solution of fenofibric acid in acetonitrile. Blank plasma samples were spiked and treated the same way as the samples. Linearity was observed between 158 μM and 0.31 μM. Method validation resulted in accuracy and precision errors of less than 5% and 8%, respectively, for a concentration of 9.8 μM. Quality control samples (9.8 μM) were included on the days of analysis and resulted in a relative standard deviation of less than 5%.

2.8. Data analysis and statistical analysis

Data from the *in vivo* study are presented as mean ± standard error of the mean (S.E.M.) for five subjects. Pharmacokinetic parameters (C_{max}, T_{max} and area under the curve (AUC)) were compared using an ANOVA test combined with a Bonferroni's multiple comparison test (logarithmic transformation of C_{max} and AUC); differences were considered statistically significant at $p < 0.05$. Regarding the *in vitro* studies, data are presented as mean ± standard deviation (S.D.). All *in vitro* experiments were performed in triplicate ($n = 3$). To determine whether or not observed differences were statistically significant ($p < 0.05$), unpaired *t*-tests were performed.

3. Results and discussion

3.1. In vivo study

Fig. 1 depicts the duodenal and systemic concentrations of fenofibrate and fenofibric acid, respectively, in fasting and postprandial conditions for Lipanthylnano® (Fig. 1A) and Lipanthyl® (Fig. 1B).

Regardless of formulation or prandial state, no dissolved fenofibrate concentrations were measured in the stomach, possibly due to the minimal amount of bile salts present in the stomach. In fasting conditions, average duodenal concentrations were clearly higher following oral administration of nano- versus microparticles: the average dose-corrected duodenal $AUC_{0-230min}$ was 3.5 times higher for nanosized fenofibrate (14.66 ± 5.01 versus 4.11 ± 0.91 μM h, $p > 0.05$) (Table 1). In four out of five volunteers, administration of nanosized fenofibrate resulted in a higher duodenal C_{max}. The average duodenal T_{max} was slightly but not significantly lower for nano- versus microsized fenofibrate (59 ± 20 versus 86 ± 25 min). Overall, duodenal concentrations did not exceed previously reported solubility data of fenofibrate, indicating that administration of micro- or nanoparticles does not generate concentrations exceeding apparent solubility of fenofibrate in FaHIF (Augustijns et al., 2014).

For all five volunteers, the plasma AUC_{0-8h} of the active metabolite fenofibric acid was higher following administration of the nanoparticles compared to the microparticles. On average, the 3.5-fold higher duodenal exposure for nano- versus microsized fenofibrate resulted in a 3.4-fold higher systemic exposure. Also the increase in average plasma C_{max} and decrease in average plasma T_{max} for the nano- versus microparticles reflected the duodenal behavior of both formulations (Table 1). Overall, the observed difference in systemic performance between Lipanthyl® and Lipanthylnano® was in line with literature data and can be attributed to the improved dissolution rate of the nanoparticles (Hanafy et al., 2007; Jia et al., 2002).

The intake of a liquid meal significantly increased duodenal fenofibrate concentrations for both formulations: compared to fasting conditions, a 10-fold increase in duodenal $AUC_{0-230min}$ was observed for the microsized formulation, whereas a 7-fold increase was observed for the nanosized formulation. As mentioned before, no dissolved fenofibrate concentrations were measured in the stomach, regardless of formulation or prandial state. The mean duodenal T_{max}-values in postprandial conditions (167 ± 17 and 155 ± 17 min for Lipanthylnano® and Lipanthyl®, respectively) were significantly increased compared to fasting conditions ($p < 0.05$). Despite the strong increase in intraluminal concentrations, the intake of food did not significantly enhance the systemic exposure for both formulations, as can be seen in Fig. 1A and B. The observed food-induced differences in plasma AUC (slight increase for microparticles, slight decrease for nanoparticles) were not statistically significant. Literature data indicate a positive food effect for the microparticles, and no food effect for the nanoparticles (Table 1) (Guivarc'h et al., 2004; Sauron et al., 2006).

The fact that the food effect on intraluminal fenofibrate concentrations cannot be translated into an effect on the systemic performance of these formulations indicates that another mechanism is affecting absorption in postprandial conditions. Different scenarios of food–drug interactions have been described in literature, alternating in a positive versus negative outcome on drug bioavailability (Schmidt and Dalhoff, 2002). In this respect, the increased amount of secreted bile, lipid degradation products and phospholipids in postprandial conditions may result in improved micellar entrapment of lipophilic drugs, leading to an increase in apparent solubility, but a decrease in drug permeability (Holmstock et al., 2013; Miller et al., 2011). This so-called solubility–permeability interplay is not uncommon for BCS class 2 and 4 compounds, with a high affinity for the hydrophobic core of mixed micelles (Amidon et al., 1982; Frank et al., 2012a; Fischer et al., 2012). For instance, despite an increased apparent solubility of the BCS class 2 model drug ABT-102 in FaSSIF compared to Hanks' Balanced Salt Solution, its permeation across the Caco-2 monolayer was not increased, due to micellar entrapment (Frank et al., 2012b). We therefore assessed the potential of fenofibrate to permeate across a membrane, starting from intestinal fluid samples aspirated in fasting and fed conditions.

Fig. 2 demonstrates the concentration accessible for absorption of fenofibrate from selected samples of HV 3, covering micro- and nanoparticles in both nutritional states. For both micro- and nanoparticles, measured concentrations of dissolved fenofibrate were higher in fed versus fasted state samples (micro: 24.61 versus 3.20 μM, nano: 123.10 versus 2.77 μM). Regardless of the higher fenofibrate concentrations in postprandial conditions, the fraction accessible for absorption appeared to be comparable to the fraction in fasting conditions. These results thus suggest that increased concentrations of fenofibrate in complex postprandial intestinal fluids do not directly enhance the driving force for absorption due to entrapment in the mixed micelles consisting of lipid degradation products, bile salts and phospholipids. This may explain the absence of a positive food effect on systemic concentrations of fenofibric acid.

3.2. In vitro simulation of fasting and postprandial fenofibrate absorption

Nowadays, the optimization of biopharmaceutical tools in order to accurately predict the *in vivo* performance of dosage forms

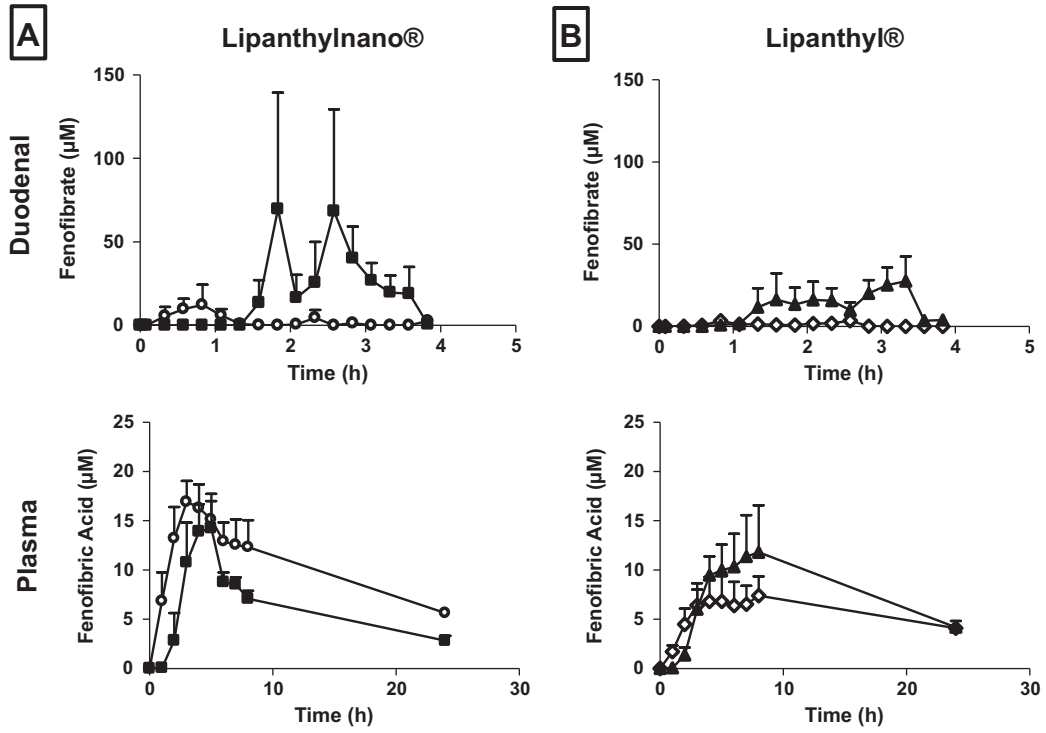

Fig. 1. (A) Duodenal (upper part) and systemic (lower part) concentration–time profiles for fenofibrate (fenofibric acid) following administration of 145 mg nanosized fenofibrate in fasted (○) and fed (■) conditions. (B) Duodenal (upper part) and systemic (lower part) concentration–time profiles fenofibrate (fenofibric acid) following administration of 200 mg microsized fenofibrate in fasted (◇) and fed (▲) conditions (mean ± S.E.M., $n = 5$).

Table 1
Mean descriptive parameters of the duodenal and systemic concentration–time profiles following administration of micro- and nanosized fenofibrate (Lipanthyl® and Lipanthylnano®) to five healthy volunteers (mean ± S.E.M.).

	Micro fasted	Micro fed	Nano fasted[a]	Nano fed[a]
Duodenal $AUC_{0-230min}$ (µM h)	4.11 ± 0.91	41.1 ± 21.2	14.7 ± 5.10	103 ± 37.2
Duodenal C_{max} (µM)	8.21 ± 2.54	44.6 ± 14.0	36.3 ± 13.5	237 ± 89.6
Duodenal T_{max} (min)	86.0 ± 25.4	155 ± 17.7	59.0 ± 20.4	167 ± 17.4
Plasma AUC_{0-8h} (µM.h)	35.8 ± 12	47.8 ± 13.4	121 ± 12.5	75.7 ± 16.3
Plasma C_{max} (µM)	7.02 ± 2.71	11.7 ± 3.94	23.2 ± 2.27	19.2 ± 3.77
Plasma T_{max} (h)	8.60 ± 3.97	9.40 ± 3.74	4.20 ± 1.11	4.40 ± 0.24

[a] Dose-corrected.

deserves considerable interest (Kostewicz et al., 2014). To achieve this goal, reference *in vivo* data is indispensable. In this study, the observed duodenal exposure for micro- and nanoparticles of fenofibrate was reflected in the systemic exposure in fasting conditions. The food-induced increase in duodenal concentrations of fenofibrate, however, was not associated with increased systemic exposure of fenofibric acid. Therefore, it can be expected that predicting the *in vivo* exposure based on the simulation of concentrations (dissolution testing) could overestimate the food effect for these formulations. Indeed, simple dissolution experiments clearly demonstrated an approximate 6-fold increase in dissolved fenofibrate concentrations in FeSSIF-V2 compared to FaSSIF for both micro- and nanoparticles (Fig. 3). As observed using aspirated intestinal fluid samples (Fig. 2), micellar encapsulation of fenofibrate in fed state conditions limits the permeation potential despite increasing concentrations. To accurately predict the behavior of micro- and nanoparticles of fenofibrate, especially in fed conditions, drug permeation should therefore be integrated in dissolution testing.

Although great efforts have recently been made to study the effect of food on intestinal absorption by using Caco-2 cells (Markopoulos et al., 2014), it is still questionable how biorelevant

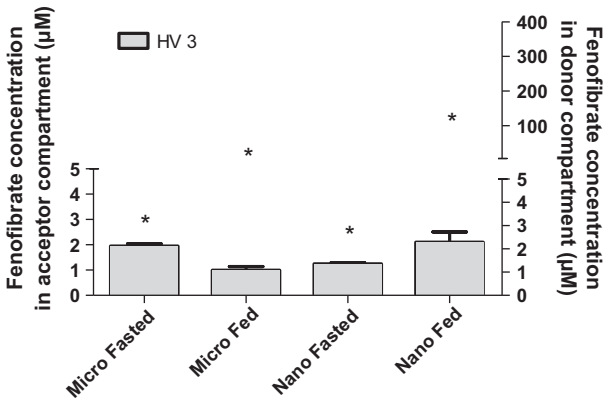

Fig. 2. Permeation potential of fenofibrate from four selected intestinal fluid samples, aspirated from HV 3 in each condition (i.e. micro- and nanosized fenofibrate in fasting and postprandial conditions). The permeation potential is expressed as the bioaccessible concentration measured after 4 h in the acceptor compartment of a dialysis setup (mean ± S.D., $n = 3$). Stars represent the dissolved concentration of fenofibrate in the selected fluids at the time of aspiration.

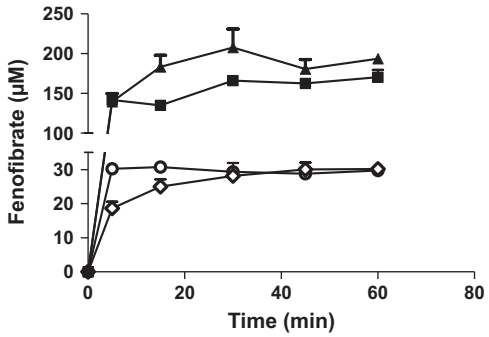

Fig. 3. Dissolution profiles of micro- (◇) and nanosized (○) fenofibrate in FaSSIF (200 ml), after transfer from FaSSGF (mean ± S.D., $n = 3$). Dissolution profiles of micro- (▲) and nanosized (■) fenofibrate in FeSSIF-V2 (200 ml), after transfer from FaSSGF (mean ± S.D., $n = 3$).

concentrations of bile salts and phospholipids can be applied in this setup without compromising the monolayer integrity. In addition, practical issues (e.g. customizable volumes, time-consuming and resource-intensive cell culture) may hamper the coupling of dissolution testing with Caco-2 permeation for early formulation evaluation. Consequently, there is a need of simple setups combining dissolution with permeation. In the present study, we simulated the effect of food on the intestinal absorption of fenofibrate by implementing a permeation bag with sink conditions (i.e. to simulate intestinal uptake) in a dissolution vessel (i.e. to simulate the intestinal lumen).

To simulate fasting and fed conditions, dissolution experiments in combination with permeation were performed by making use of FaSSGF and FaSSIF & $FeSSGF_{Fortimel}$ and FeSSIF-V2, respectively. The use of Fortimel Extra® to prepare $FeSSGF_{Fortimel}$ is in accordance with the liquid meal administered in the *in vivo* study. The formulations were allowed to disintegrate for 15 min in 50 ml of simulated gastric fluids, followed by transfer to 150 ml of simulated intestinal fluids (4-fold dilution). As a function of time, samples were taken from the dissolution vessel and from the permeation bag. Fig. 4 depicts the measured concentrations of fenofibrate in the dissolution vessel and in the permeation bag for Lipanthyl® and Lipanthylnano® in fasting conditions. No fenofibrate dissolution was observed in FaSSGF or $FeSSGF_{Fortimel}$, in line with the *in vivo* situation.

Considering the apparent solubility of fenofibrate in FaSSIF (26.6 ± 3.8 µM) (Augustijns et al., 2014), neither of the formulations generated concentrations exceeding this solubility. Only a

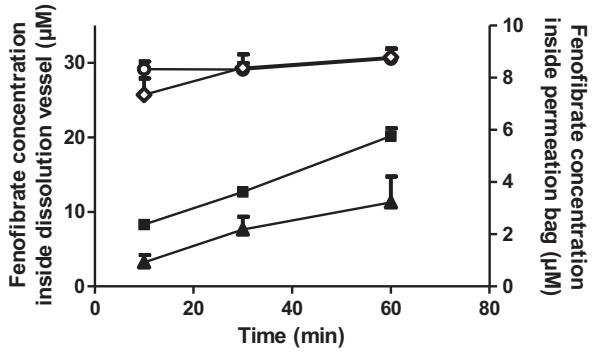

Fig. 4. Dissolution and permeation of micro- and nanosized fenofibrate in FaSSIF using a dissolution vessel with sink permeation bag. Fenofibrate concentrations inside the dissolution vessel are indicated by ○ (nano) and ◇ (micro). Fenofibrate concentrations inside the permeation bag are indicated by ■ (nano) and ▲ (micro) (mean ± S.D., $n = 3$).

relatively small difference in dissolution kinetics could be observed between micro- and nanoparticles. It is, however, worth mentioning that the dissolution kinetics will depend on the specifications of the dissolution setup. For example, in a USP Apparatus 2 (paddle rotation speed set at 75 rpm), the solubility of fenofibrate was still not reached after 60 min dissolution of microsized particles (Zuo et al., 2013). In our study, applying a magnetic stirrer with a rotation speed of 400 rpm, the solubility was already achieved after 30 min (Fig. 4), presumably due to altered hydrodynamics and a stronger comminution mechanism.

Regarding the fenofibrate concentrations inside the permeation bag after one hour, an approximate two-fold increase in concentration was observed in favor of the nanoparticles, which is in line with the ratio of plasma C_{max} between Lipanthylnano® and Lipanthyl®, as seen in the *in vivo* study (Table 1). The implementation of an absorptive sink in dissolution testing is thus required to simulate the dynamic interplay of dissolution and absorption and allows for an improved discriminative power between micro- and nanosized fenofibrate.

To simulate formulation performance in postprandial conditions, the same setup was applied, with the exception of using fed state instead of fasted state simulated media. Two sets of experiments were performed to demonstrate if the presence of a liquid meal is required to predict the food effect on fenofibrate absorption. In a first set of experiments, postprandial conditions were simulated without the presence of a liquid meal. Both formulations resided for 15 min in 50 ml of FaSSGF and, subsequently, the content was transferred to 150 ml of FeSSIF-V2. After transfer, concentrations of fenofibrate were measured inside the dissolution vessel and inside the permeation bag (Fig. 5). A comparison between fed and fasted state results was made in order to assess a possible food effect.

Inside the dissolution vessel, fenofibrate concentrations from both formulations were strongly increased in fed conditions, in line with the *in vivo* situation. The approximately 6-fold increase in fenofibrate concentrations, observed for both formulations after 60 min, seemed to enhance the driving force for passive diffusion through the permeation bag, resulting in higher concentrations inside the acceptor compartment compared to fasting conditions. *In vivo*, however, the food-induced increase in duodenal fenofibrate concentrations was not accompanied with a similar increase in systemic exposure. This suggests that the *in vitro* setup with an absorptive sink but without a liquid meal does not capture the impact of the micellar entrapment observed *in vivo*.

In order to further optimize our setup, Fortimel Extra® was added to FaSSGF in a 1:1 ratio, in order to become $FeSSGF_{Fortimel}$, as described by Jantratid et al. (Jantratid et al., 2008). Employing this setup, fenofibrate concentrations inside the dissolution vessel were still enhanced in fed conditions (Fig. 6). Remarkably, the presence of this liquid meal resulted in a proper distinction between dissolution behavior of both formulations, as also observed *in vivo*; the two-fold increase of fenofibrate concentrations starting from nanoparticles compared to microparticles are in accordance with a similar increase of duodenal C_{max} and $AUC_{0-230min}$ (as depicted in the mean concentration-time profiles, Fig. 1). Inside the permeation bag, however, a non-significant decrease in fenofibrate concentrations was observed compared to fasting state conditions: after 60 min, fenofibrate concentrations were 2.1-fold lower for the nanoparticles, and 1.7-fold lower for the microparticles ($p > 0.05$). In agreement with the *in vivo* situation, assessing the permeation potential did not reveal a significant food effect on fenofibrate absorption, despite increased intraluminal concentrations.

These results clearly demonstrate that the use of a liquid meal is critical to simulate the impact of micellar entrapment on postprandial fenofibrate absorption. The formed patterned colloidal species (i.e. micelles, uni- and mulitlamellar vesicles) can upload a high

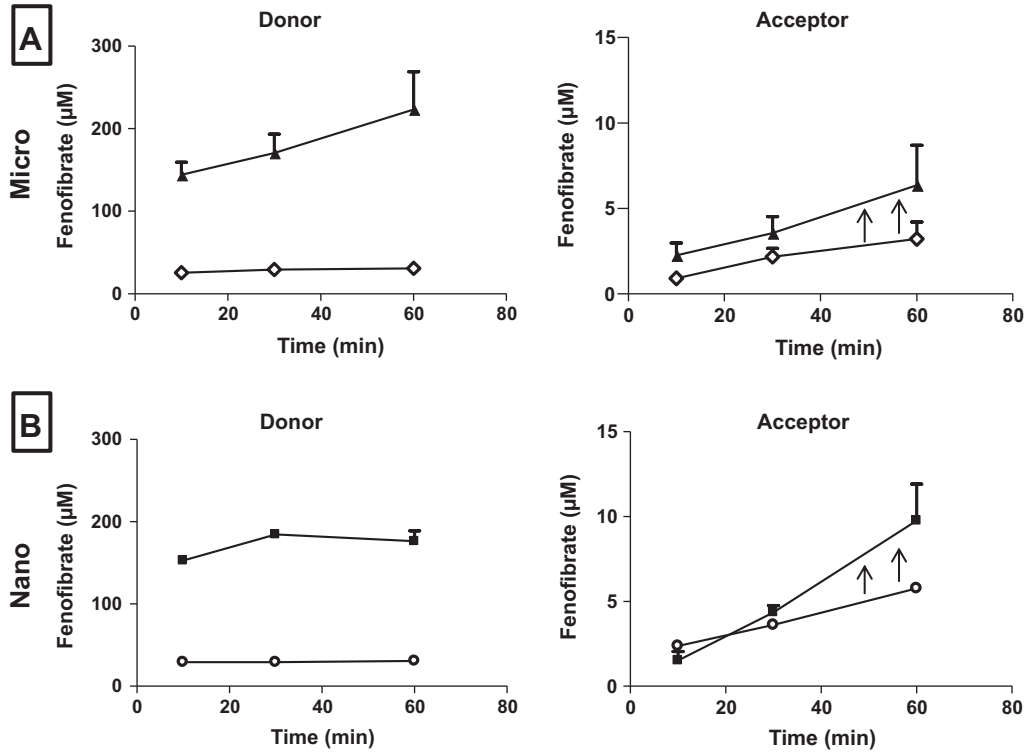

Fig. 5. (A) Dissolution and permeation of microsized fenofibrate in FeSSIF-V2 following transfer from FaSSGF, using a dissolution vessel with sink permeation bag. Fenofibrate concentrations in the dissolution vessel (i.e. donor) and in the permeation bag (i.e. acceptor) in fed conditions are shown by (▲). For comparison purposes, fasted state results are indicated by (◇). (B) Dissolution and permeation of nanosized fenofibrate in FeSSIF-V2 following transfer from FaSSGF, using a dissolution vessel with sink permeation bag. Fenofibrate concentrations in the dissolution vessel (i.e. donor) and in the permeation bag (i.e. acceptor) are shown by (■). For comparison purposes, fasted state results are indicated by (○) (mean ± S.D., $n = 3$).

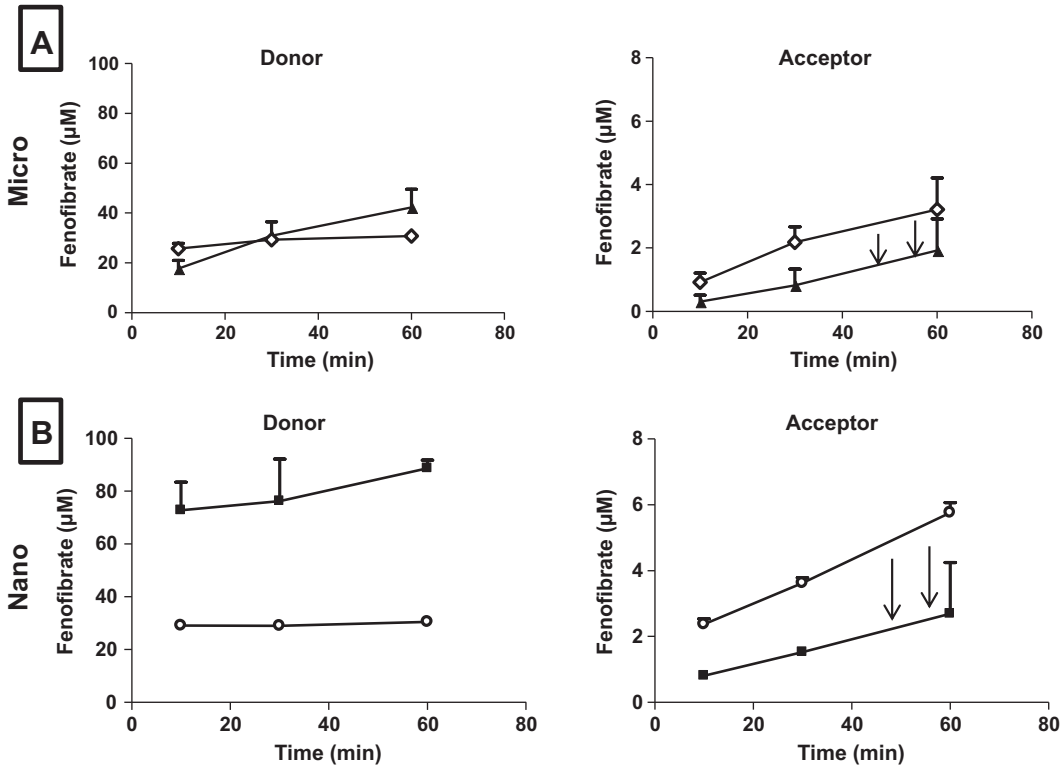

Fig. 6. (A) Dissolution and permeation of microsized fenofibrate in FeSSIF-V2 following transfer from $FeSSGF_{Fortimel}$, using a dissolution vessel with sink permeation bag. Fenofibrate concentrations in the dissolution vessel (i.e. donor) and in the permeation bag (i.e. acceptor) are shown by (▲). For comparison purposes, fasted state results are indicated by (◇). (B) Dissolution and permeation of nanosized fenofibrate in FeSSIF-V2 following transfer from $FeSSGF_{Fortimel}$, using a dissolution vessel with sink permeation bag. Fenofibrate concentrations in the dissolution vessel (i.e. donor) and in the permeation bag (i.e. acceptor) are shown by (■). For comparison purposes, fasted state results are indicated by (○) (mean ± S.D., $n = 3$).

amount of drug, resulting in an increased apparent solubility (Porter et al., 2007). However, the high affinity of a lipophilic drug to the core of these species may reduce the fraction accessible for absorption (i.e. bioaccessible fraction) compared to fasting conditions (Holmstock et al., 2013; Stappaerts et al., 2014). To conclude, the combination of $FeSSGF_{Fortimel}$ and FeSSIF-V2 in a simple dissolution/permeation setup enables the qualitative prediction of postprandial fenofibrate absorption.

4. Conclusion

For the first time, this study simultaneously monitored the intraluminal behavior and systemic exposure of micro- and nano-sized fenofibrate in man. The results clearly demonstrate that enhancing the concentration of lipophilic drugs in complex intestinal fluids is not always reflected in improved absorption. Especially in postprandial conditions, the encapsulation of a lipophilic drug in micelles and vesicles may limit the drug's permeation potential despite increasing intraluminal concentrations (solubility–permeability interplay). Whereas a full mechanistic understanding requires an in-depth analysis of the dynamic equilibrium between free and encapsulated drug, we introduced dissolution testing using biorelevant media in combination with permeation assessment into a sink permeation bag as a simple yet pragmatic approach to capture this interplay in early formulation evaluation.

Acknowledgments

This work has received support from (1) the Institute for the Promotion of Innovation through Science and Technology in Flanders (IWT) and (2) the Innovative Medicines Initiative Joint Undertaking (http://www.imi.europa.eu) under Grant Agreement No. 115369, resources of which are composed of financial contribution from the European Union's Seventh Framework Program and EFPIA companies' in kind contribution. We also would like to thank Nancy Haesendonck, Marleen Hellemans, Kathy Van Herck, Karolien Van Langendonck and Hilde Van Gucht (Gastroenterology, University Hospitals Leuven, Belgium) for their assistance during the *in vivo* studies.

References

Amidon, G.E., Higuchi, W.I., Ho, N.F.H., 1982. Theoretical and experimental studies of transport of micelle-solubilized solutes. J. Pharm. Sci. 71, 77–84.
Amidon, G.L., Lennernäs, H., Shah, V.P., Crison, J.R., 1995. A theoretical basis for a biopharmaceutic drug classification: the correlation of in vitro drug product dissolution and in vivo bioavailability. Pharm. Res. 12, 413–420.
Augustijns, P., Wuyts, B., Hens, B., Annaert, P., Butler, J., Brouwers, J., 2014. A review of drug solubility in human intestinal fluids: implications for the prediction of oral absorption. Eur. J. Pharm. Sci. 57, 322–332.
Benet, L.Z., Broccatelli, F., Oprea, T.I., 2011. BDDCS applied to over 900 drugs. AAPS J. 13, 519–547.
Brouwers, J., Brewster, M.E., Augustijns, P., 2009. Supersaturating drug delivery systems: the answer to solubility-limited oral bioavailability? J. Pharm. Sci. 98, 2549–2572.
Buckley, S.T., Frank, K.J., Fricker, G., Brandl, M., 2013. Biopharmaceutical classification of poorly soluble drugs with respect to "enabling formulations". Eur. J. Pharm. Sci. 50, 8–16.
Fischer, S.M., Buckley, S.T., Kirchmeyer, W., Fricker, G., Brandl, M., 2012. Application of simulated intestinal fluid on the phospholipid vesicle-based drug permeation assay. Int. J. Pharm. 422, 52–58.
Frank, K.J., Rosenblatt, K.M., Westedt, U., Hölig, P., Rosenberg, J., Mägerlein, M., Fricker, G., Brandl, M., 2012a. Amorphous solid dispersion enhances permeation of poorly soluble ABT-102: true supersaturation vs. apparent solubility enhancement. Int. J. Pharm. 437, 288–293.
Frank, K.J., Westedt, U., Rosenblatt, K.M., Hölig, P., Rosenberg, J., Mägerlein, M., Brandl, M., Fricker, G., 2012b. Impact of FaSSIF on the solubility and dissolution-/permeation rate of a poorly water-soluble compound. Eur. J. Pharm. Sci. 47, 16–20.
Guivarc'h, P.-H., Vachon, M.G., Fordyce, D., 2004. A new fenofibrate formulation: results of six single-dose, clinical studies of bioavailability under fed and fasting conditions. Clin. Ther. 26, 1456–1469.
Hanafy, A., Spahn-Langguth, H., Vergnault, G., Grenier, P., Tubic Grozdanis, M., Lenhardt, T., Langguth, P., 2007. Pharmacokinetic evaluation of oral fenofibrate nanosuspensions and SLN in comparison to conventional suspensions of micronized drug. Adv. Drug Deliv. Rev. 59, 419–426.
Holmstock, N., Bruyn, T.D., Bevernage, J., Annaert, P., Mols, R., Tack, J., Augustijns, P., 2013. Exploring food effects on indinavir absorption with human intestinal fluids in the mouse intestine. Eur. J. Pharm. Sci. 49, 27–32.
Jantratid, E., Janssen, N., Reppas, C., Dressman, J.B., 2008. Dissolution media simulating conditions in the proximal human gastrointestinal tract: an update. Pharm. Res. 25, 1663–1676.
Jia, L., Wong, H., Cerna, C., Weitman, S.D., 2002. Effect of nanonization on absorption of 301029: ex vivo and in vivo pharmacokinetic correlations determined by liquid chromatography/mass spectrometry. Pharm. Res. 19, 1091–1096.
Juenemann, D., Jantratid, E., Wagner, C., Reppas, C., Vertzoni, M., Dressman, J.B., 2011. Biorelevant in vitro dissolution testing of products containing micronized or nanosized fenofibrate with a view to predicting plasma profiles. Eur. J. Pharm. Biopharm. 77, 257–264.
Kostewicz, E.S., Abrahamsson, B., Brewster, M., Brouwers, J., Butler, J., Carlert, S., Dickinson, P.A., Dressman, J., Holm, R., Klein, S., Mann, J., McAllister, M., Minekus, M., Muenster, U., Müllertz, A., Verwei, M., Vertzoni, M., Weitschies, W., Augustijns, P., 2014. In vitro models for the prediction of in vivo performance of oral dosage forms. Eur. J. Pharm. Sci. 57, 342–366.
Lipinski, C.A., 2000. Drug-like properties and the causes of poor solubility and poor permeability. J. Pharmacol. Toxicol. Methods 44, 235–249.
Markopoulos, C., Thoenen, F., Preisig, D., Symillides, M., Vertzoni, M., Parrott, N., Reppas, C., Imanidis, G., 2014. Biorelevant media for transport experiments in the Caco-2 model to evaluate drug absorption in the fasted and the fed state and their usefulness. Eur. J. Pharm. Biopharm. 86, 438–448.
Miller, J.M., Beig, A., Krieg, B.J., Carr, R.A., Borchardt, T.B., Amidon, G.E., Amidon, G.L., Dahan, A., 2011. The solubility–permeability interplay: mechanistic modeling and predictive application of the impact of micellar solubilization on intestinal permeation. Mol. Pharm. 8, 1848–1856.
Nakarani, M., Misra, A.K., Patel, J.K., Vaghani, S.S., 2010. Itraconazole nanosuspension for oral delivery: formulation, characterization and in vitro comparison with marketed formulation. Daru 18, 84–90.
Porter, C.J.H., Trevaskis, N.L., Charman, W.N., 2007. Lipids and lipid-based formulations: optimizing the oral delivery of lipophilic drugs. Nat. Rev. Drug. Discov. 6, 231–248.
Sauron, R., Wilkins, M., Jessent, V., Dubois, A., Maillot, C., Weil, A., 2006. Absence of a food effect with a 145 mg nanoparticle fenofibrate tablet formulation. Int. J. Clin. Pharmacol. Ther. 44, 64–70.
Schmidt, L.E., Dalhoff, K., 2002. Food–drug interactions. Drugs 62, 1481–1502.
Sigfridsson, K., Lundqvist, A.J., Strimfors, M., 2011. Particle size reduction and pharmacokinetic evaluation of a poorly soluble acid and a poorly soluble base during early development. Drug Dev. Ind. Pharm. 37, 243–251.
Stappaerts, J., Wuyts, B., Tack, J., Annaert, P., Augustijns, P., 2014. Human and simulated intestinal fluids as solvent systems to explore food effects on intestinal solubility and permeability. Eur. J. Pharm. Sci. 63, 178–186.
Van Eerdenbrugh, B., Vermant, J., Martens, J.A., Froyen, L., Humbeeck, J.V., Van den Mooter, G., Augustijns, P., 2010. Solubility increases associated with crystalline drug nanoparticles: methodologies and significance. Mol. Pharm. 7, 1858–1870.
Wang, Y., Zhang, D., Liu, Z., Liu, G., Duan, C., Jia, L., Feng, F., Zhang, X., Shi, Y., Zhang, Q., 2010. In vitro and in vivo evaluation of silybin nanosuspensions for oral and intravenous delivery. Nanotechnology 21, 155104.
Williams, H.D., Trevaskis, N.L., Charman, S.A., Shanker, R.M., Charman, W.N., Pouton, C.W., Porter, C.J.H., 2013. Strategies to address low drug solubility in discovery and development. Pharmacol. Rev. 65, 315–499.
Zuo, B., Sun, Y., Li, H., Liu, X., Zhai, Y., Sun, J., He, Z., 2013. Preparation and in vitro/in vivo evaluation of fenofibrate nanocrystals. Int. J. Pharm. 455, 267–275.